SPE 131737

Reduced-Variables Method for General-Purpose Compositional Reservoir Simulation

Huanquan Pan and Hamdi A. Tchelepi, SPE, Stanford University

This paper was prepared for presentation at the CPS/SPE International Oil & Gas Conference and Exhibition in China held in Beijing, China, 8–10 June 2010.

Abstract

Compositional flow simulation is necessary for planning EOR (Enhanced Oil Recovery) and CO_2 sequestration projects. We refer to the standard approach for performing the Phase Equilibrium (PE) computations as the Conventional-Variables (CV) method. In compositional simulation, the cost of PE calculations increases dramatically as the number of components increases, and the PE computations can become the most time consuming part of a simulation run. To reduce the number of components, lumping procedures are used, but that often entails the loss of possibly important phase-behavior information. The Reduced-Variables (RV) method is a robust and efficient scheme for PE calculations. However, there is limited information regarding the performance of RV in practical compositional flow simulation (i.e., coupled flow, transport, and thermodynamics). For example, there is only one published work with small 2D IMPEC (IMplicit Pressure, Explicit Compositions) simulations. Here, we integrated the RV method with a General Purpose Research Simulator (GPRS). This modular, object-oriented, computational framework allows us to make direct performance comparisons of RV- and CV-based compositional simulations. We use five different fluids, ranging from 6 to 26 components, and we focus on challenging multi-contact miscible displacements. We use two reservoir models: the first is the top layer of the SPE10 problem, and the second is a Discrete Fracture Model (DFM) with unstructured grids. The RV-based simulations are significantly more efficient than state-of-the-art CV-based computations. For the problems we describe here, the RV-based PE calculations can be up to seven times more efficient than the standard (CV-based) approach, and the total simulation time using RV can be a quarter of that used by the standard method. We show that the cost of the RV method for PE calculations is a linear function of the number of reduced variables, and we show that the total simulation time using RV is a weak function of the number of components used to describe the fluid. These properties of the RV approach enable us to study complex EOR processes in large-scale reservoir models, where large numbers of components and grid blocks are required. We propose that general-purpose simulators use the RV approach for the PE computations associated with large-scale compositional simulations.

Introduction

Compositional flow simulation is used to study EOR processes, such as multi-contact miscible gas injection. Compositional simulators usually employ the assumption of instantaneous thermodynamic equilibrium, and they use an Equation of State (EOS) to describe the phase behavior. In reservoir engineering applications, a widely used simplification is that only the two hydrocarbon phases (liquid and vapor) are involved in the complex component mass transfer, and that the water phase is simple. During a compositional flow simulation, PE calculations are required for each cell at each time step. For a given overall composition, pressure, and temperature in a cell, the PE computations associated with flow simulation consist of: (1) Phase-Stability Analysis (PSA) for a single-phase hydrocarbon mixture, and (2) Two-Phase Flash (TPF) calculations for a two-phase hydrocarbon mixture.

In a general-purpose compositional reservoir simulator that uses the natural variables (Coats et al. 1998), the PE computations can be split into PSA and TPF as follows. If a cell was in a two-phase state during the previous Newton iteration, the new (for the current Newton iteration) phase-state is determined from the gas- or oil- saturation; the saturation fields are obtained by solving the linearized flow (component mass-conservation) equations (i.e., solving the reduced Jacobian). Note that the reduced Jacobian is obtained from the global Jacobian system, which includes the full set of linearized equations, including the fugacity constraints.

For each Newton iteration, we loop over all the cells in the model. If a cell was in a single-phase (liquid, or vapor) state in the previous iteration, PSA is performed to determine if the mixture is stable. PSA is usually performed twice with a vapor-like and a liquid-like mixture. If the PSA results indicate that the single-phase hydrocarbon mixture in the cell is stable, there is no need to perform further PE calculations for this cell during the current Newton iteration. If, on the other hand, the PSA results indicate that the mixture is unstable (i.e., likely to form two phases), then the fugacity-equality relations of the cell are linearized and added to the global Jacobian, which also includes the linearized flow equations and associated constraints. Solution of the global system entails performing TPF calculations and solving the coupled flow equations. The TPF calculations yield the composition and amount of the vapor and liquid phases. It is important to note that in a typical compositional simulation run, TPF computations are needed only for those cells that change their phase-state from one to two phases between Newton iterations, or time steps.

In general, the percentage of cells that require TPF computations is small. Our experience with the GPRS simulator (Cao 2002, Jiang 2007), which employs the natural-variables formulation, is that less than 5% of the PE computations are TPFs and the remainder is for PSA. Thus, the efficiency and robustness of the PSA kernel plays a crucial rule in the overall efficiency of a compositional flow simulation.

In the standard Conventional Variables (CV) method, for a mixture with Nc components, Nc-1and Nc variables are required for PSA and TPF computations, respectively. Iterative methods are used to solve the highly nonlinear equations for both PSA and TPF, and these PE calculations end up consuming a significant fraction of the total simulation time in reservoir models with large numbers of components. One approach to reduce the PE computational cost involves lumping the components into a smaller number of pseudo-components. However, the component lumping approach can lead to significant errors in capturing important aspects of the phase behavior, especially around the critical region. Another strategy to reduce the computational cost is the use of equilibrium ratios (K-values) tables for the pressure (and temperature) ranges of interest (Coats, 1985). The K-value table look-up method can be quite effective as long as the compositional dependence of the K-values is weak, and this assumption is rarely valid for complex multi-contact (miscible) gas-injection processes of practical interest. Stenby and Wang (1993) proposed a non-iterative method for TPF calculations, which can be quite effective. However, as we mentioned above, in a general-purpose simulator, the PE cost is dominated by PSA not TPF. Thus, improving the efficiency of PE computations for mixtures with large numbers of components, especially the PSA part, is necessary for accurate modeling of complex EOR processes in highly detailed reservoir models.

The RV method was proposed by Michelsen (1986) for a mixture, where the Binary Interaction Coefficient (BIC), $k_{i,j,}$ is zero for all the components. Later, several efforts were aimed at relaxing this restriction on $k_{i,j}$ (Jensen and Fredenslund 1987, Hendriks and van Bergen 1992, Kaul and Thrasher 1996). However, these efforts targeted the TPF (i.e., flash) computations; as a result, the overall savings due to using RV were small compared to the standard CV method. The advantage of the RV approach for PSA was demonstrated clearly by Firoozabadi and Pan (2002). They showed that the Newton method is globally convergent in the RV space, which is a highly desirable property for PSA. Pan and Firoozabadi (2003) then demonstrated that the nonlinear behavior of the Gibbs free-energy functions for TPF calculations is significantly better (smaller number of iterations) in the RV space compared with the CV space. Similar findings were made recently by Okuno, et al. (2008). These highly desirable properties provide strong motivation for the RV method to replace CV-based approaches for PE calculations in compositional simulation.

Nitchita et al. (2006) extended the RV approach to mixtures that can form three hydrocarbon phases. Hoteit and Firoozabadi (2006) studied the discontinuous Tangent Plane Distance (TPD) problem in RV space. Li and Johns (2006) proposed an RV method that uses two sets of parameters to replace the BICs. With their approach, the number of reduced variables is five for PSA and six for TPF calculations, regardless of the BIC values. Methods that use BICs are very widely used, and transforming these models into another parameter set is likely to prove quite difficult in practice.

Recall that in the natural-variables formulation, for cells with two hydrocarbon phases the thermodynamic equilibrium equations, which consist of the fugacity equality between the vapor and liquid phases for each component in the mixture, are used as constraints when solving the nonlinear flow equations. We have found that in many cases, use of relatively loose PE residual tolerances, especially for mixtures in the vicinity of the critical region, can lead to severe convergence problems in the global Newton loop, and can often be a major cause for timestep cuts.

Because the coupling between flow, transport, and thermodynamics in compositional displacement processes is highly nonlinear and quite complex, the robustness and efficiency of the RV method must be demonstrated for challenging simulations, including multi-contact miscibility, large numbers of components, wide variations in pressure and composition, and large time steps. For this purpose, the RV method is integrated with GPRS (Cao, 2002, Jiang, 2007). Here, we use Fully Implicit Method (FIM) with the natural-variables (Coats, 1998) formulation.

In recent, there have been several efforts aimed at improving the efficiency of compositional flow simulation. For example, Rasmussen et al. (2006) proposed empirical criteria to bypass the PSA computation in parts of the compositional space. Voskov and Tchelepi (2009a, 2009b) developed the Compositional Space Adaptive Tabulation (CSAT) method to speed up the PE computations associated with compositional flow simulation. In CSAT, tables of tie-lines and critical tie-lines are collected and updated adaptively. These tie-line tables are then used to speed-up both the PSA and TPF computations. Note that acceleration, or

preconditioning, techniques such as CSAT, rely on having a robust method to (1) generate and adaptively update the tables, and (2) perform PSA around complex phase boundaries (Voskov and Tchelepi 2009a, 2009b). Thus, the RV method can also replace the standard CV method to improve the performance of CSAT and similar methods.

Most of the RV studies reported in the literature were performed as stand-alone PE calculations. To our knowledge, few RV-based compositional flow simulation studies have been published. Wang and Barker (1995) applied the Michelsen (1986) zero BICs method in a compositional simulator. Honami et al. (2000) studied mixtures, where only one component has a k_{ij} value not equal to zero. Okuno et al. (2008) applied the Li and Johns (2006) method in the IMPEC-based UT-COMP simulator in a reservoir model with 400 cells. For general-purpose reservoir simulation, a practical RV method should not modify the given fluid characterization, or the BIC values, specified by the user. We follow such a 'black-box' RV approach based on a general Principal Component Analysis (PCA) strategy (Hendriks and van Bergen 1992, Firoozabadi and Pan 2002, Pan and Firoozabadi 2003). We integrated the RV module, which honors the user-specified EOS model and data exactly, into the GPS simulator (Cao 2002, Jiang 2007), and we demonstrate the performance of this RV-based simulation framework for several simulation problems of practical interest.

Brief Description of the RV Method

The modified Peng-Robinson equation of state (Robinson and Peng, 1978) is used for the study. The van der Waals mixing rules of the two-parameter EOS are

$$a = \sum_{i=1}^{N_C}\sum_{j=1}^{N_C}\sqrt{a_i}\sqrt{a_j}(1-k_{ij})x_i x_j \qquad (1)$$

$$b = \sum_{i=1}^{N_C} b_i x_i \,, \qquad (2)$$

where the matrix $\bar{\mathbf{k}} = [1-k_{ij}]_{i,\,j=1,\ldots N_C}$ is symmetric and can be expressed as

$$\bar{\mathbf{k}} = \mathbf{S}\mathbf{D}\mathbf{S}^T \,. \qquad (3)$$

Here, **D** is a diagonal matrix with elements equal to the eigenvalues λ_i (i=1,….Nc) of the $\bar{\mathbf{k}}$ matrix. The matrix ***S*** is

$$\mathbf{S} = \left(\mathbf{q}^{(1)} \quad \mathbf{q}^{(2)} \quad . \quad . \quad \mathbf{q}^{(\alpha)} \quad . \quad . \quad \mathbf{q}^{(N_C)}\right), \qquad (4)$$

where $\mathbf{q}^{(\alpha)}$ is the corresponding eigenvector of λ_α, $\mathbf{q}^{(\alpha)} = \left(q_{\alpha_1} \quad q_{\alpha_2} \quad . \quad . \quad . \quad q_{\alpha_N}\right)^T$. From Eq. 3, one obtains

$$\bar{k}_{ij} = (1-k_{ij}) = \sum_{\alpha=1}^{N_C}\lambda_\alpha \mathbf{q}_i^{(\alpha)}\mathbf{q}_j^{(\alpha)} \,. \qquad (5)$$

Substitution of Eq. 5 into Eq. 1 yields

$$a = \sum_{\alpha=1}^{N_C}\lambda_\alpha Q_\alpha^2 \,, \qquad (6)$$

where

$$Q_\alpha = \sum_{i=1}^{N_C} q_\alpha^{'} x_i \qquad (\alpha = 1, 2, \ldots\ldots, M). \qquad (7)$$

In Eq. 7, $q_\alpha^{'} = \sqrt{a_i}\,q_\alpha$.

Using PCA, the parameter a can be approximated using a small number of principal components, namely,

$$a \approx \sum_{\alpha=1}^{M}\lambda_\alpha Q_\alpha^2 \,. \qquad (8)$$

The number of principal components (eigenvalues and associated eigenvectors), M, required to obtain an accurate approximation is usually small compared with the number of components (chemical species) used to represent the fluid mixture, N_c. So, working with the reduced variables will be quite effective when $M << N_C$.

Algorithms for Phase Equilibrium Calculations

Pan and Firoozabadi (Firoozabadi and Pan 2002, Pan and Firoozabadi 2003) used minimization of the TPD for PSA and for the Gibbs free-energy function associated with TPF computations. They used a Lagrange-multiplier approach, and the minimization was achieved by iteration on these multipliers. We have found that iteration on the nonlinear equations cast in RV space leads to

the same robustness and performance as the Lagrange-multiplier approach, but that the implementation is simpler. Therefore, direct iteration in RV space is used here. For the RV-based computations for PSA, we use the Newton method. On the other hand, for the TPF calculations in RV space, we use a combined SSI-Newton method. We start with SSI (successive substitution iteration), and switch to Newton's method when a particular residual threshold is reached. Note that the combined SSI-Newton method is used for both PSA and TPF calculations in the CV method. The details of the SSI-Newton scheme can be found in previous papers (Firoozabadi and Pan 2002, Pan and Firoozabadi 2003, Hoteit and Firoozabadi 2006). In the combined SSI-Newton method of this study, the threshold value of the residual for switching between SSI and Newton's method is adjusted automatically, whenever the Newton step is out of the physical range of any variable. This strategy improves the overall performance.

In both CV and RV methods, we encountered convergence problems of the Newton loop for PSA computations in regions where the TPD is discontinuous (Hoteit and Firoozabadi 2006). Hoteit and Firoozabadi (2006) suggested that the physical region of the reduced variables be checked during each Newton iteration, and to then switch to SSI if any reduced variable is out of the physical region. We tried this strategy and found that it works quite well, but that it is too expensive in compositional flow simulation. For example, for the SPE5 fluid, thousands of SSI iterations are needed in some cells. Here, we monitor the residual change during the iterations to solve the problem.

We emphasize that the simulation results presented here compare CV and RV based compositional simulations that share the exact input data, and that we do not modify the user-input models and parameters. Moreover, use of RV is only for the PE computations of PSA and TPF, and we do not reformulate, or transform, the variables in the flow (mass conservation) equations.

Reservoir Fluids in Case Studies

Five reservoir fluids are used in this study: (1) **SPE3**: 9-component, gas-condensate fluid in the near-critical region (Kenyon and Behie 1983). (2) **SPE5**: 6-component hydrocarbon-oil away from the critical region. This is a simple fluid taken from the SPE5 problem (Killough and Kossack 1987). (3) **Condenate1**: 8-component, gas-condensate fluid. (4) **Condensate2**: Kilgrin gas-condensate mixed with a 5% mole-fraction of H_2S. This condensate includes all non-hydrocarbon components: N_2, CO_2 and H_2S in reservoir fluids. (5) **Oil1**: 26-component, reservoir oil. The details of these fluids are given in **Tables 1**-**5**. **Table 6** lists the non-zero eigenvalues calculated from the ($\mathbf{1-k_{ij}}$) matrix for the five fluids. These eigenvalues are ordered in decreasing order according to their absolute value. The eigenvalues used in the RV based simulations are shown in red in **Table 6**.

Stand-alone Calculation Results

To compare the performance of the CV and RV methods, a new C++ software module was developed to perform the stand-alone PSA and TPF calculations. Note that all computations in this work were executed using a PC with 3.0 GHz CPU and 1.95 GB of RAM. **Fig. 1** shows the execution time vs. M (number of eigenvalues used) for the SPE3 fluid, where 22,000 PSA and 6,000 TPF computations were performed. The pressure varied from 4,400 psia (single phase) to 700 psia (two phases). The execution time of the CV method is 28 seconds. As shown later, for flow simulations using this fluid, three eigenvalues are sufficient (see **Fig. 6**). In **Fig. 1**, the execution time is 2.2 seconds for the RV method with three eigenvalues. So, in this stand-alone test, compared with CV computations, the RV approach leads to a speed up of one-order of magnitude. **Fig. 2** plots the execution time vs. the number of components (Nc) with 36,000 PSA and 9,000 TPF computations for the SPE5 fluid. To increase Nc, the heavy C_{7+} components were evenly divided. All three non-zero eigenvalues are retained in the computations. As Nc increases, the execution time increases quite slowly for the RV approach. For example, the time for the 10-component mixture is only 40% more than that for the 6-component mixture. However, for the CV method, the computational time increases rapidly with the number of components. In this case, the computational cost of the 10-component mixture is almost twice as much as that for the 6-component one.

Before Pan and Firoozabadi's work (2002, 2003), people attributed the performance of the RV method to having fewer variables. As demonstrated above, this is partially true. However, the improved nonlinear behavior of the TPD functions in RV space plays a crucial rule in the speedup of the PE calculations. Moreover, the Gibbs free-energy function is also smoother in RV space compared to that in CV space. For example, for the near-critical SPE3 fluid, we can switch from SSI to Newton at a larger residual threshold when using RV compared with CV. In **Fig. 1**, the execution time increases linearly with M because of the improved nonlinear character of the TPD and the Gibbs free-energy functions in RV space. The number of iterative variables with M=7 in the RV method is the same as the number in the CV method, but the execution time is 4.6 seconds in RV space and 28 seconds for the CV method. The SPE3 fluid is in the critical region, and the combined SSI-Newton scheme for the PSA computations struggles in the CV space. On the other hand, quadratic convergence of the Newton method is realized in the RV space.

Simulation Results

We tested the first four fluids described earlier using the top layer of the SPE 10 problem (Reservoir I), which has 220 x 60 =13,200 cells. The permeabilities of Kx (Ky=Kx), Kz and the porosities of the reservoir are plotted in **Figs. 3, 4** and **5**. One

injection well is located in cell (1,1,1) and one production well in (220,60,1). The injection stream is the separator gas of the reservoir fluid at standard conditions. Both wells are operated under BHP controls. GPRS with FIM with a maximum timestep of 50 days is used for all the flow simulations presented here.

In the following figures Mi (i=1, 2, 3, …) represents the results from the RV method with Mi being the number of eigenvalues used in the computations, and CV denotes the results from the standard conventional variables method. "EOS" refers to the execution time of the PE computations, and "Other" denotes the total time minus the "EOS" time. Most of the "Other" time comes from assembling the Jacobian matrix and linear-solution of the flow equations.

SPE3: Fig. 6 compares the results of the oil and gas production and gas-injection rates using CV and M3 methods, respectively. These simulated results are very close to each other. **Fig. 7** and **Fig. 8** plot the pressure and the gas saturation distributions in the model for these two methods at 1800 days. **Fig. 9** shows the execution time for the different methods. To study the effect of M on the simulation cost, we use M values up to nine (note that $\lambda_8 = \lambda_9 = 0$, see **Table 6**). The "EOS" time increases almost linearly with M, which is similar to the stand-alone results (see **Fig. 1**). The "Other" time is independent M and is almost constant. Note that we only replace the conventional variables with reduced variables in the PE computations. Thus, the other computations do not change; therefore, the time for "Other" (on a per Newton iteration basis) should change very little across the various methods. SPE3 is a near-critical fluid, the PSA computations using the CV method are quite slow, while the RV method achieves excellent efficiency. The RV method leads to significant gains in the overall simulation time. The "EOS" time for M3 is 398 seconds vs. 2712 seconds for the CV method. So, in this case M3 is almost seven times as fast as the CV method for PE computations in the simulations. The number of iterative variables for the PE calculations in M7 is same as the number in the CV method, but the execution time of M7 is much less than that of the CV method. The results reveal the superior nonlinear behavior of the TPD and Gibbs free-energy functions in RV space compared with the CV-based approach. **Fig. 10** shows the effect of the number of components in the mixture, N_c on the execution time using the SPE3 fluid. In these computations, the C_{7+} components are evenly divided to increase Nc. As N_c increases, the "EOS" time increases slowly in the M4 case compared with the CV results. When Nc increases from 9 to 13, the EOS time for M4 increases from 491 to 678 seconds, which is equivalent to 47 seconds per component. On the other hand, the rate of increase is 435 seconds per component for the CV method. Therefore, the "EOS" time using the RV method with M=4 is almost 10 times faster than the CV method. As expected, for the given Nc, the "Other" time in the M4 case is almost the same as that of the CV method. In **Fig. 10**, the slightly larger "Other" time for the M4 case is due to one, or two, more time steps compared with the CV-based simulation. Note that the results of the well flow rates, pressure and gas saturation distributions are very close to each other for all the simulations.

SPE5: **Fig. 11** plots the oil and gas production and gas injection rates with the CV method and M2. The results of M2 are in good agreement with those of the CV method. **Fig. 12** shows the "EOS" and the "Other" time for the various cases. The SPE5 fluid is a six-component hydrocarbon oil away from the critical point. Thus, the phase behavior associated with the SPE5 fluid is much simpler than the cases involving the SPE3 fluid. With the SPE5 case, the "EOS" time for the CV method is only 30% of the total simulation time. The SPE5 fluid has three non-zero eigenvalues (see **Table 6**), and the M3 case yields the same results as the CV method. However, note that the "EOS" time for the M3 simulation is less than that for the CV method. **Fig. 11** indicates that the M2 case has enough accuracy for the flow simulations, and the "EOS" time in M2 is 60% of the CV method. For this case, the eigenvalues λ_4, λ_5, and λ_6 are zero. So, the simulation results of M3, M4, M5, M6 and the CV method are practically identical. These results indicate that the "EOS" time increases linearly with M, and the "Other" time is almost constant for all methods. The execution time vs. the number of components, where the heavy fraction is evenly divided, is plotted in **Fig. 13**. The "EOS" time increases by 106 seconds from 6 to 11 components for the M3 simulations, while the time is 836 seconds for the CV based simulation. The "Other" time is about the same for the CV and RV simulations.

Condensate1: as shown in **Fig. 14**, the M3 simulation gives results that agree quite well with the CV method. **Fig. 15** compares the execution time for the different approaches. Similar to the results for the SPE3 and SPE5 fluids, the "EOS" time increases linearly with M for the RV method, and the "Other" time is almost constant for all approaches. The "EOS" time in M3 is only 60% of the CV-method time.

Condensate2: the mixture includes all non-hydrocarbon components: N_2, CO_2 and H_2S in reservoir fluids. These components have relatively large k_{ij} values, which can significantly affect the size of the eigenvalues. The dominant eigenvalues are used as reduced variables. There are 8 non-zero eigenvalues for the 15-component mixture. The results of the M4 case are accurate enough, in terms of the flow behaviors. **Fig. 16** shows good agreement in the gas and oil production and gas-injection rates between M4 and the CV method. **Fig. 17** and **Fig. 18** show good agreement of the cell pressures and gas saturations between M4 and the CV method. **Fig. 19** plots the execution time for the different methods. Note that there are 8 non-zero eigenvalues for the mixture, and

the simulation results from M8 to M14 and the CV method are practically the same. When M is less than 7, the "EOS" time increases slowly, then a little faster when M is larger than 7. The "Other" time is the same for all approaches, as expected.

Oil1: there are 11 non-zero eigenvalues for this 26-component mixture. The simulation is conducted in a fractured reservoir (Reservoir II). A discrete fracture model (DFM) is used with 5,000 cells, which have highly heterogeneous properties. The permeability and porosity are 0.1 md and 0.25 for the matrix, while they are 1,000,000 md and 1.0 for the fractures. The largest cell pore-volume is more than 1000 ft^3 and the smallest is less than 10^{-6} ft^3. There are two wells: one injector and one producer, and both wells employ BHP control. The details of the DFM reservoir model and the wells are described by Gong et al. (2007). **Fig. 20** shows good agreement of the gas and oil production and the gas injection rates between M3 and the CV method. **Fig. 21** compares the execution time for the different approaches. When M increases in RV, the "EOS" time increases slowly. The "Other" time is almost the same among all methods. Overall, M3 is twice as fast as the CV method.

This oil was also characterized into 6 components. The simulation results of the 26- and 6-component characterizations are plotted in **Fig. 22** for the CV method. The discrepancies of the gas injection rate, the gas and oil production rates are 24%, 8%, and 13%, respectively, at 10 years. The differences in the cumulative injection and production are quite large for 10 years. This highlights the importance of using an appropriate number of components in describing the compositional effects.

RV vis. Non-iterative Approaches

Rasmussen et al. (2006) divided the phase diagram into three regions and proposed empirical criteria to bypass the PSA in the single-phase region, where the TPD is equal to zero, or the PSA solution is trivial. But, the standard CV method is still used in the other two regions, as well as, in the TPD=0 region if the proposed criteria are not satisfied. We believe that Rsumssuen's strategy is likely to prove quite useful.

Here, we followed a different approach, in which the RV method, as opposed to the standard CV approach, is used to perform the PE computations needed by CSAT. In general, we expect that replacing CV with RV in CSAT should improve the performance, especially for a difficult, near-critical, fluid like SPE3. We found that the RV-based CSAT simulations always much more efficient compared with their CV-based CSAT counterparts. **Fig. 23** compares the CPU time for M3, CV, CSAT (CV-based) and CSAT-M3 (RV-based) approaches for simulations using the SPE3 fluid in Reservoir I. The "EOS" time is reduced from 419 seconds using CSAT to just 32 seconds when CSAT is combined with the RV method with M=3. The "EOS" time in the CSAT-M3 case is only 1.2% of the time taken by the standard CV method. As a result, CSAT-M3 brings down the total simulation time from 3261 seconds in the standard CV method to only 544 seconds.

In a general-purpose simulator, the natural-variables formulation may perform better than other formulations (Voskov and Tchelepi 2009c), especially if large time steps (i.e., high throughput, large saturation changes) are employed. As discussed in the Introduction, the convergence tolerances used for the TPF computations have a direct impact on the performance of the global Newton loop, especially for a near-critical fluid. Our experience also indicates that using loose tolerances in conjunction of table look-up methods, for either PSA or TPF calculations, usually leads to more global Newton iterations and often to smaller time steps, on average. The RV method is a fast and iterative method to replace the standard approach and does not cause problems in solving the flow equations, and it is extremely robust and efficient for near-critical fluids.

Determination of the Number of Eigenvalues

There is in no simple rule one can follow to determine how many principal eigenvalues should be used for the flow simulations. From our analysis, we believe that the appropriate number of eigenvalues to use depends strongly on the phase-behavior of the fluid and the solution path of the displacement process in compositional space. Moreover, we expect the dependence on the reservoir properties (permeability, porosity, etc.) to be weak. We have conducted several simulations in homogenous reservoir models. **Table 7** lists the properties of these models and the well locations. Both injection and production wells are operated under BHP control. The injection stream is the separator gas of the reservoir fluid at standard conditions. **Fig. 24** plots the results for SPE3, **Fig. 25** for SPE5, and **Fig. 26** for Condensate2. From these figures, we find that the minimum number of eigenvalues is 3 for SPE3, 2 for SPE5, and 4 for Condensate2. These numbers are exactly the same as those that lead to highly accurate simulation results in the SPE10 top layer.

We also found that if any eigenvalue whose absolute value is larger than 0.07 is kept in the computation, the simulation results of the RV method have excellent agreement with those of the CV method for all the test cases. So, we recommend that any eigenvalue with $|\lambda_\alpha| > 0.07$ be kept in the RV method. This approach may be too conservative, for example, $|\lambda_4|$ in SPE3 and Oil1 are both larger than 0.07 (see **Table 6**), but dropping these eigenvalues in the RV-based simulations does not affect the simulation results. To obtain an optimal number of eigenvalues, simple simulations in a homogenous model with hundreds of cells and with different M values should be conducted with the reservoir fluid, as we did for the SPE3, SPE5, and Condensate2 fluids.

Conclusion Remarks

Using the reduced variables method to deal with the phase equilibrium calculations in compositional flow simulation is more robust and much more efficient than the conventional-variables approach. This is because there are fewer iterative variables and better nonlinear behavior of the tangent plane distance and the Gibbs free-energy functions. Our extensive case studies show that the execution time of the phase equilibrium calculations, which include phase stability analysis and two-phase flash computations, is significantly reduced when the RV method is used for all the cases we tested. For a reservoir fluid in the critical region, like the SPE3 case, the RV method is several-fold faster than the conventional-variables method for the phase-equilibrium computations in the GPRS simulator.

It is often the case that a large number of components is needed to represent the phase behavior accurately in an EOR process. Since the simulation time using the reduced-variables method increases slowly with the number of components used to represent the fluid system, the reduced-variables approach is recommended as the default strategy for general-purpose compositional simulation of practical problems. To determine the number of eigenvalues used in a simulation, we recommend dropping any eigenvalue of the $(1 - k_{ij})$ matrix, whose absolute value is less than 0.07. Simple reservoir simulations can be used to tune the optimal number of eigenvalues to use in large-scale flow simulations.

Table 1-Composition and non-zero BICs for SPE3

Comp.	Mol%	$k_{CO_2-C_i}$	$k_{N_2-C_i}$	$k_{C_1-C_i}$	$k_{C_2-C_i}$	$k_{C_3-C_i}$
CO2	1.21					
N2	1.94					
C1	65.99	0.1	0.036			
C2	8.69	0.13	0.05			
C3	5.91	0.135	0.08			
C4-6	9.67	0.1277	0.1002	0.09281		
C7+1	4.745	0.1	0.1	0.130663	0.006	0.006
C7+2	1.515	0.1	0.1	0.130663	0.006	0.006
C7+3	0.33	0.1	0.1	0.130663	0.006	0.006

Table 2-Composition and non-zero BICs for SPE5

Comp.	Mol%	$k_{C_1-C_i}$	$k_{C_3-C_i}$
C1	50		
C3	3		
C6	7		
C10	20		
C15	15	0.05	0.005
C20	5	0.05	0.005

Table 3-Nnon-zero BICs for Condensate1

Comp.	$k_{C_1-C_i}$	$k_{CO_2-C_i}$	$k_{C_2-C_i}$	$k_{C_3-C_i}$	$k_{C_4-C_i}$
C1					
CO2	0.1				
C2	0	0.13			
C3	0	0.135			
C4	0	0.13			
C8	0.0129	0.1153	0.0103	0.0077	0.0052
C15	0.0453	0.0908	0.0363	0.0272	0.0161
C20+	0.0676	0.074	0.0541	0.0406	0.027

Table 4-Composition and non-zero BICs for Condensate2

Comp.	Mol%	$k_{N_2-C_i}$	$k_{CO_2-C_i}$	$k_{H_2S-C_i}$	$k_{C_1-C_i}$
N2	0.1805				
CO2	0.959501	-0.02			
H2S	4.999858	0.17	0.1		
C1	82.16562	0.12	0.093	0.08	
C2	2.356004	0.12	0.128	0.06	
C3	1.216002	0.12	0.123	0.06	
iC4	0.684001	0.12	0.136	0.06	0.02
nC4	0.351501	0.12	0.125	0.06	0.02
iC5	0.209	0.12	0.131	0.06	0.025
nC5	0.133	0.12	0.12	0.06	0.025
C6+	0.947911	0.12	0.12	0.06	0.035
C10+	1.196052	0.12	0.12	0.06	0.038
C15+	1.170497	0.12	0.12	0.06	0.038
C20+	0.857281	0.12	0.12	0.06	0.038
C25+	2.573269	0.12	0.12	0.06	0.038

Table 5-Non-zero BICs for Oil1

Comp.	$k_{H_2S-C_i}$	$k_{CO_2-C_i}$	$k_{N_2-C_i}$	$k_{C_1-C_i}$	$k_{C_2-C_i}$	$k_{C_3-C_i}$
H2S						
CO2	0.097					
N2	0.165	-0.02				
C1	0.085	0.1	0.036			
C2	0.075	0.13	0.05	0.002		
C3	0.075	0.135	0.085	0.007	0.001	
IC4	0.06	0.13	0.095	0.012	0.003	
NC4	0.06	0.13	0.095	0.012	0.003	
IC5	0.06	0.125	0.095	0.017	0.004	0.001
NC5	0.06	0.125	0.095	0.018	0.005	0.002
C6	0.1	0.125	0.1	0.0096	0.01	0.01
C7	0.1	0.125	0.1	0.0135	0.01	0.01
C8	0.1	0.125	0.1	0.0164	0.01	0.01
C9	0.1	0.125	0.1	0.019	0.01	0.01
C10	0.1	0.125	0.1	0.0212	0.01	0.01
C11	0.1	0.125	0.1	0.023	0.01	0.01
C12	0.1	0.125	0.1	0.0247	0.01	0.01
C13	0.1	0.125	0.1	0.0261	0.01	0.01
C14	0.1	0.125	0.1	0.0275	0.01	0.01
C15	0.1	0.125	0.1	0.0288	0.01	0.01
C16	0.1	0.125	0.1	0.0299	0.01	0.01
C17	0.1	0.125	0.1	0.031	0.01	0.01
C18	0.1	0.125	0.1	0.0317	0.01	0.01
C19	0.1	0.125	0.1	0.0325	0.01	0.01
C23	0.1	0.125	0.1	0.0349	0.01	0.01
C39	0.1	0.125	0.1	0.0414	0.01	0.01

Table 6-Non-zero eigenvalues

Fluid	SPE3	SPE5	Oil1	Condensate1	Condensate2
Nc	9	6	26	8	15
M=1	8.58646	5.96356	25.3917	7.72341	14.4582
2	0.332337	0.070228	0.438499	0.210068	0.417943
3	0.193246	-0.03379	0.185387	0.0983027	0.120496
4	-0.09432		0.087738	-0.0297065	0.0715114
5	-0.0233		-0.07572	-0.00186464	-0.0517508
6	0.009158		-0.03192	-0.00147071	-0.0191591
7	-0.00359		0.02191	0.00127023	0.00272196
8			-0.01892	-5.57E-06	
9			0.001546		
10			-0.00021		
11			-1.49E-05		

Table 7-Reservoir properties and well locations for simple simulations			
Fluid	SPE3	SPE5	Condensate2
Dimension (ft x ft x ft)	10000x1000x50	15000x15000x100	10000x1000x50
Number of Cells	10x10x5	30x30x3	10x10x5
Kx (mD)	100	100	100
Ky (mD)	100	100	100
Kz (mD)	10	25	10
porosity	0.1	0.3	0.1
W-I location*	(1,1,1)	(1,1,1)	(1,1,1)
W-P location*	(10,10,5)	(30,30,3)	(10,10,5)

*W-I: Injection Well W-P: Production Well

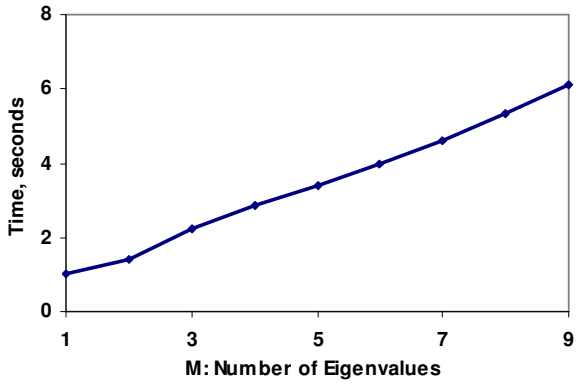

Fig. 1 CPU time vs. M for SPE3.

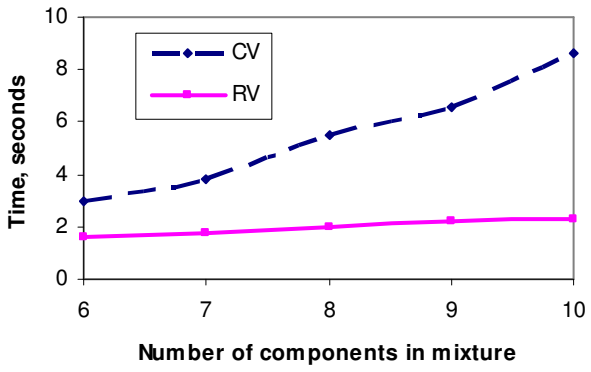

Fig. 2 CPU time vs. number of components for SPE5.

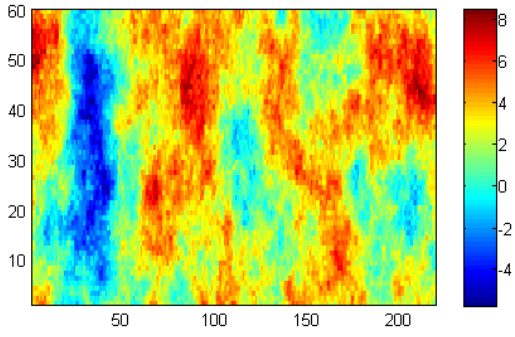

Fig. 3-Permeability logKx of Reservoir I.

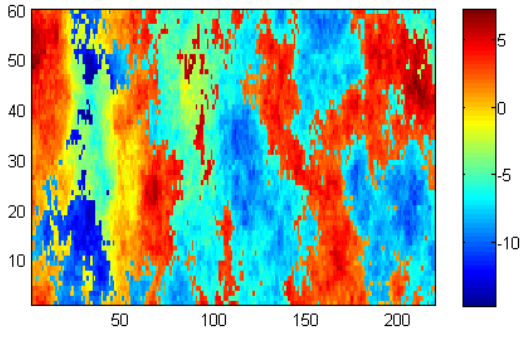

Fig. 4-Permeability logKz of Reservoir I.

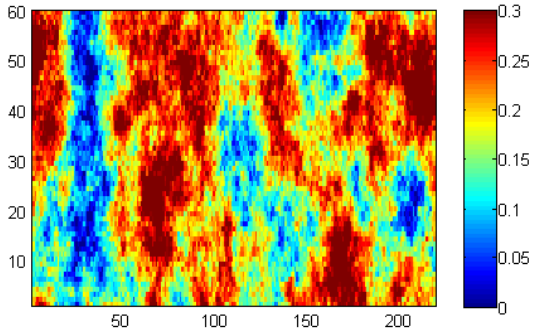

Fig. 5-Porosity of Reservoir I.

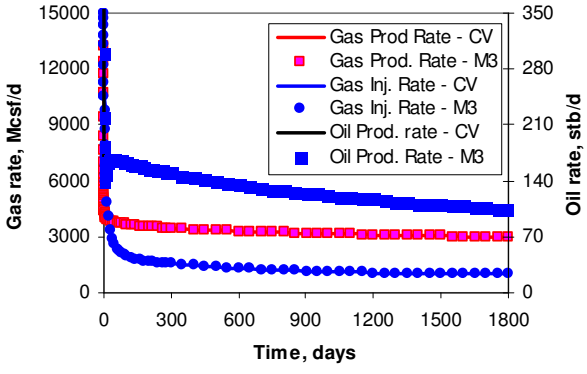

Fig. 6 Well flow rate for SPE3 fluid.

Fig. 7-Pressure distribution of Reservoir I for SPE3 at 1800 days using CV (left) and M3 (right).

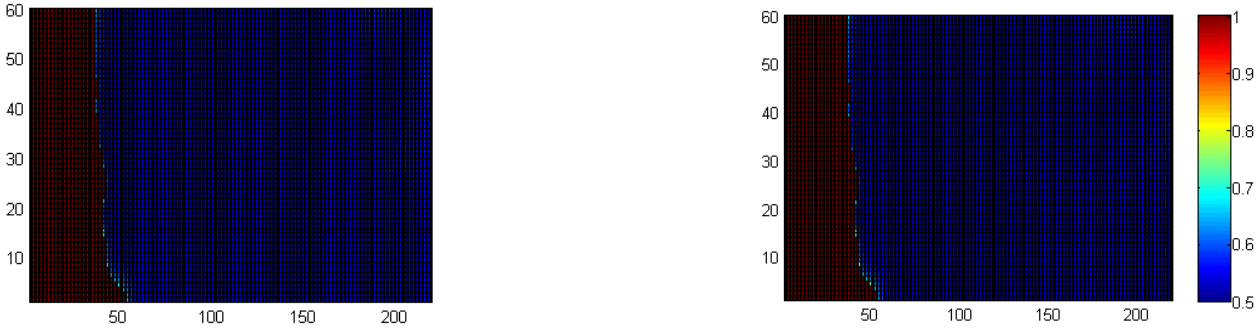

Fig. 8- Gas saturation distribution of Reservoir I for SPE3 at 1800 days using CV (left) and M3 (right).

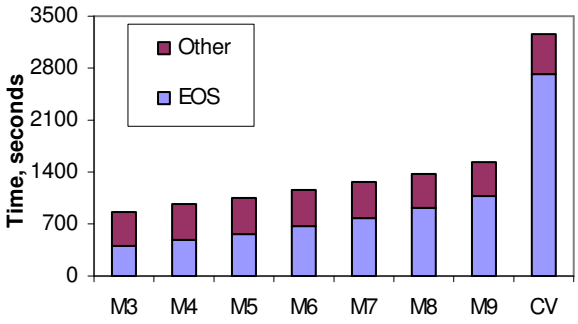

Fig. 9 Execution time in different approaches for SPE3.

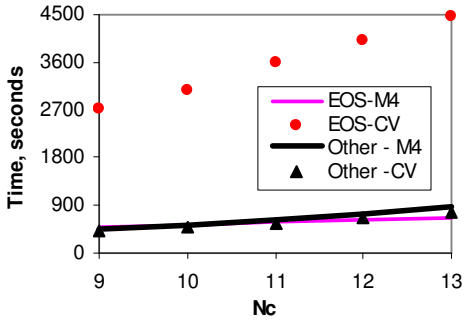

Fig. 10 Execution time vs. Nc for SPE3.

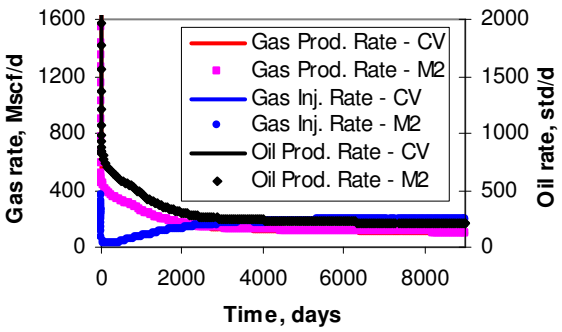

Fig. 11-Well flow rate for SPE5.

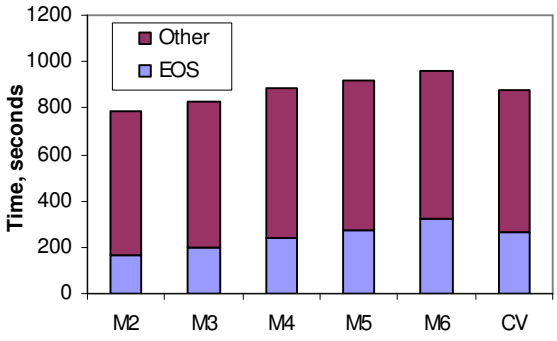

Fig. 12-Execution time in different approaches for SPE5.

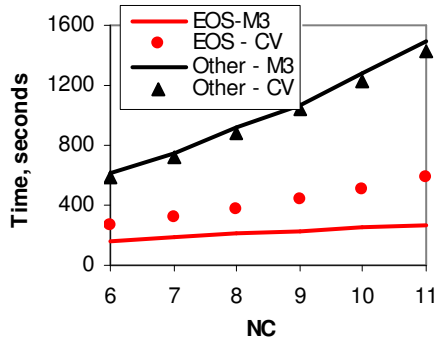

Fig. 13-Execution time vs. Nc for SPE5 fluid

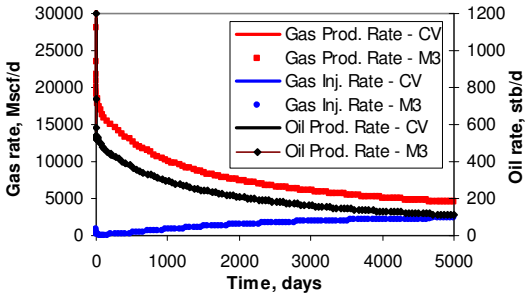

Fig. 14-Well flow rate for Condensate1

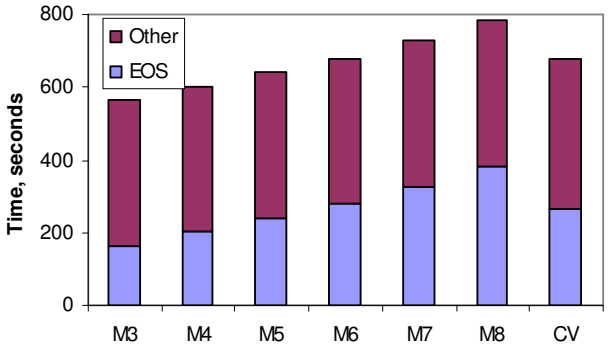

Fig. 15-Execution time in different approaches for Condensate1.

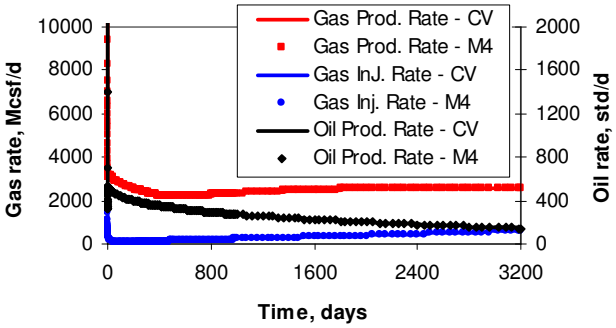

Fig. 16-Well flow rate for Condensate2.

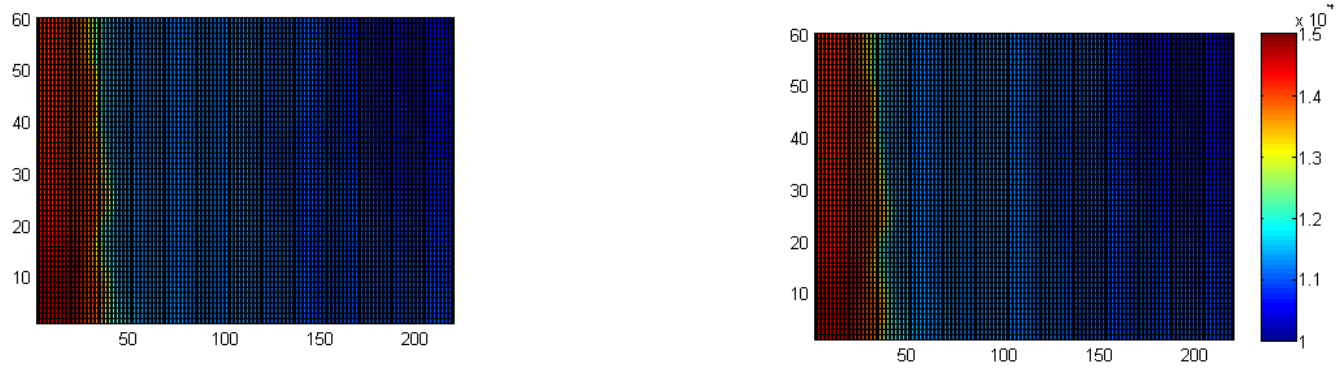

Fig. 17-Pressure distribution of Reservoir I for Condensate2 at 3200 days using CV (left) and M4 (right).

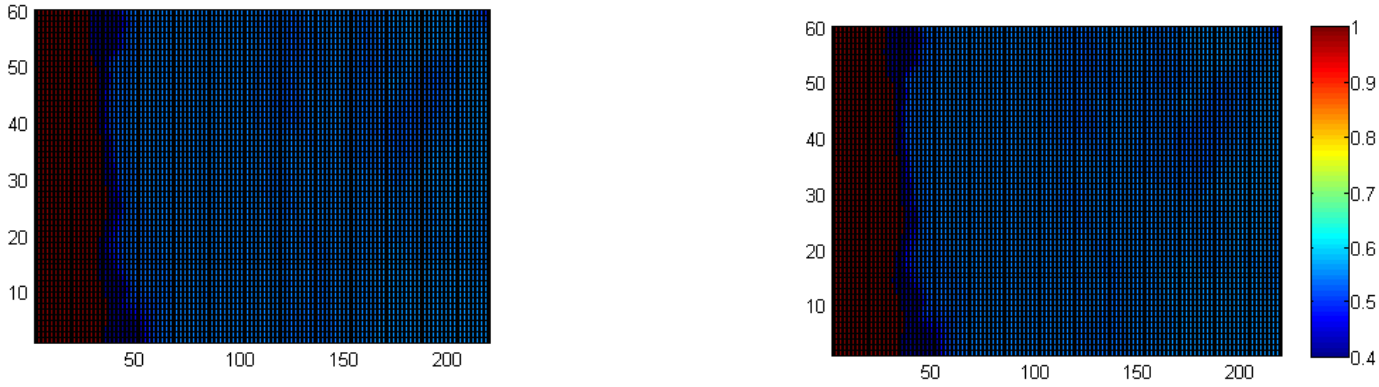

Fig. 18-Gas saturation distribution of Reservoir I for Condensate2 at 3200 days using CV (left) and M4 (right).

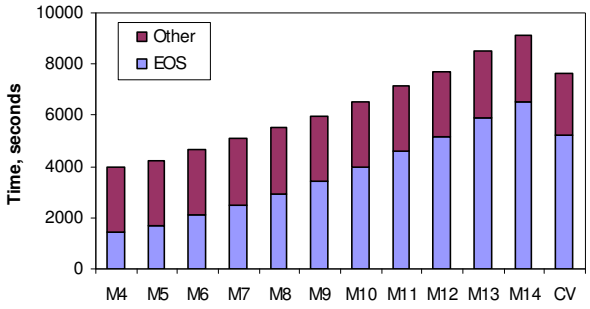

Fig. 19-Execution time in different approaches for Condensate2.

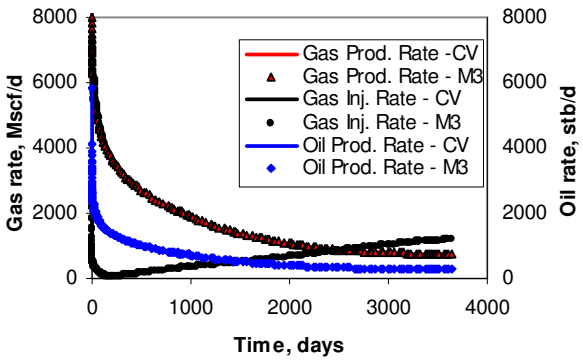

Fig. 20-Well flow rate for Oil1.

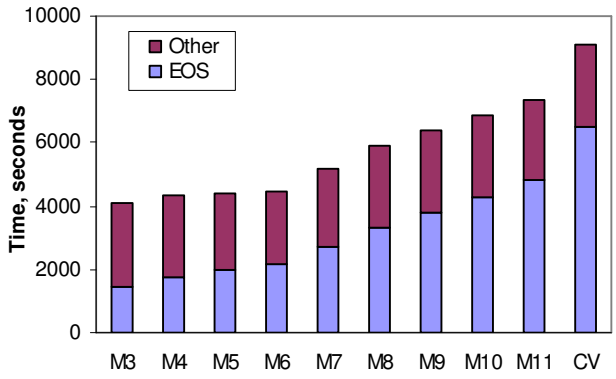

Fig. 21-Execution time in different approaches for Oil1.

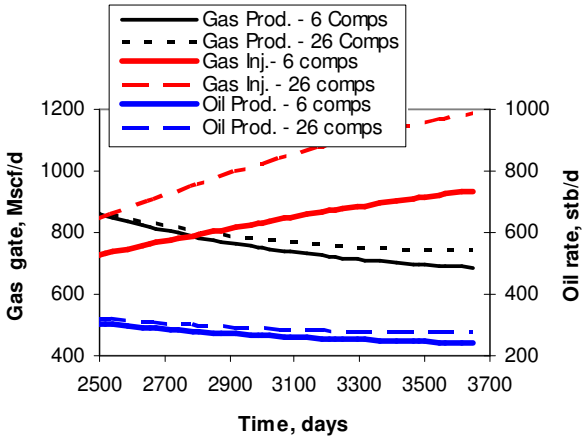

Fig. 22 Well flow rate for Oil1 with 6 and 26 components.

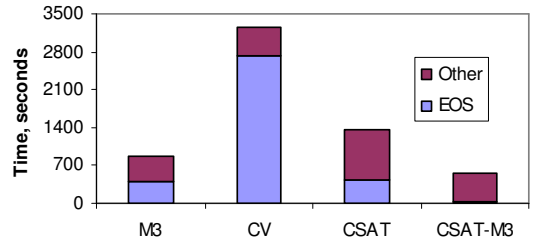

Fig. 23-CPU time comparison for SPE3.

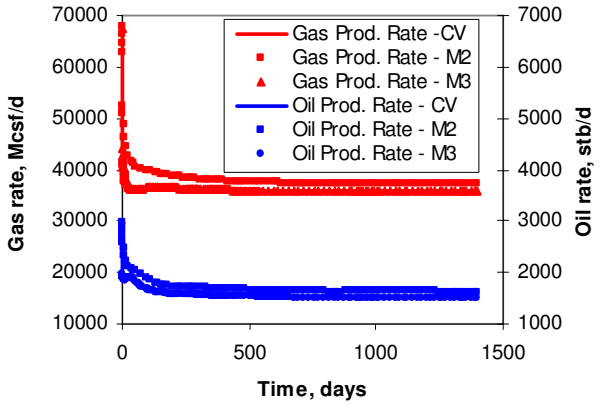

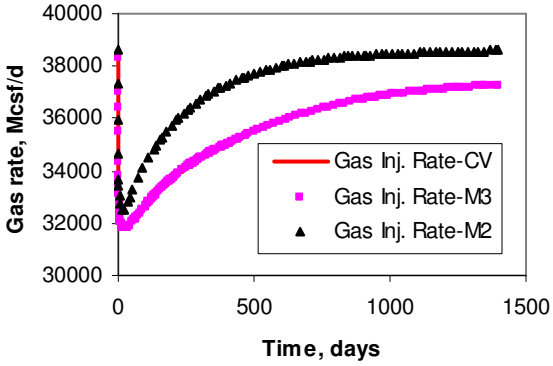

Fig. 24-Well flow rate for SPE3 in a simple reservoir.

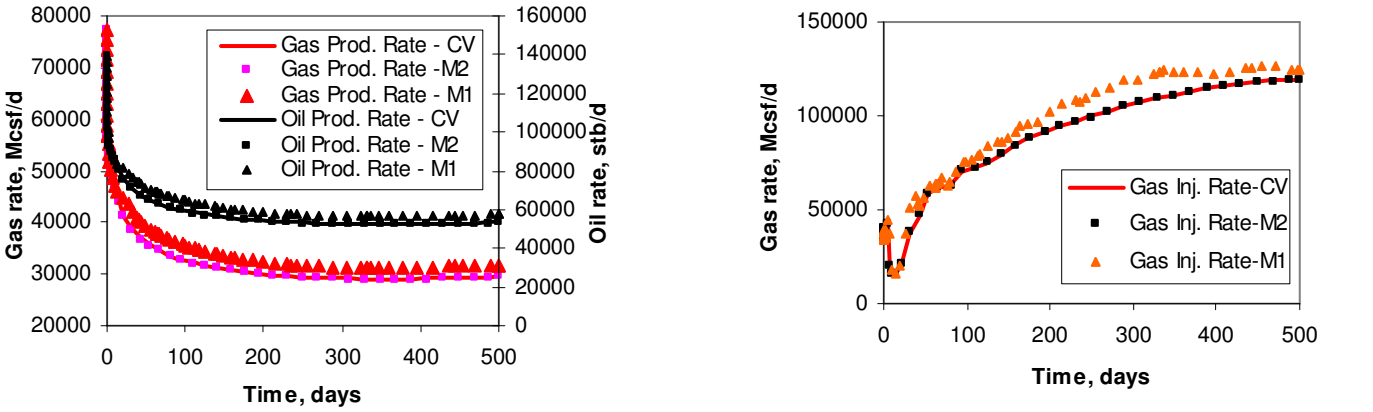

Fig. 25- Well flow rate for SPE5 in a simple reservoir.

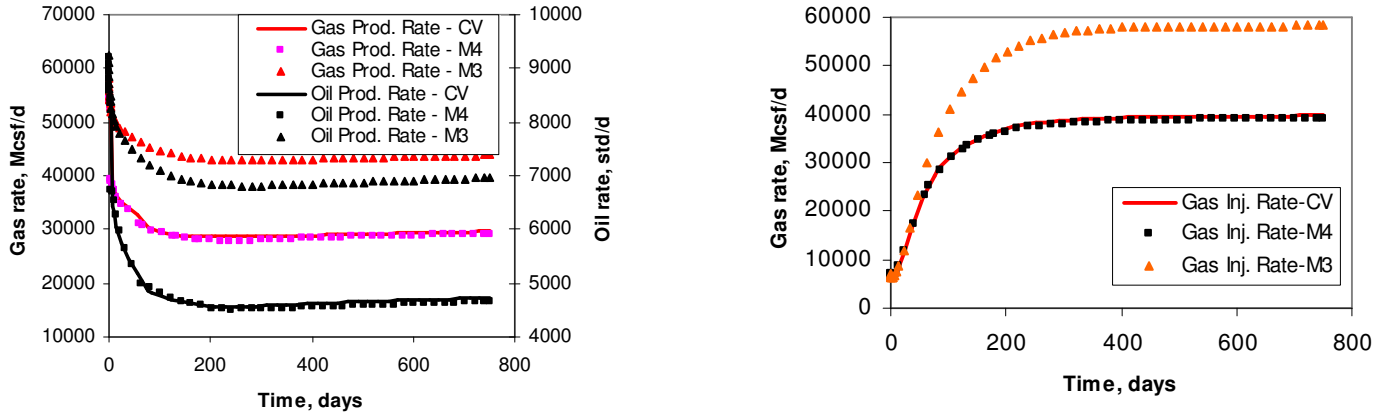

Fig. 26- Well flow rate for Condensate2 in a simple reservoir.

Nomenclature

a	EOS parameter for a mixture
a_i	EOS parameter for component i
b	EOS parameter for a mixture
b_i	EOS parameter for component i
D	diagonal matrix with diagonal elements of eigenvalues
k_{ij}	binary interaction coefficient between components i and j
$\bar{k}_{ij}$	$=(1-k_{ij})$
M	number of eigenvalues used in simulation
Mi	total i eigenvalues used in simulation
Nc	number of components in a mixture
$\mathbf{q}^{(\alpha)}$	corresponding eigenvector of λ_α
Q_α	reduced variable defined in Eq. 7
S	matrix of eigenvectors defined in Eq. 4
x_i	mole fraction of component i in a mixture
λ_α	eigenvalue

Abbreviations

BIC	binary interaction coefficient
CSAT	Compositional Space Adaptive Tabulation
CV	Conventional Variable

DFM Discrete Fracture Model
EOR Enhanced Oil Recovery
EOS Equation of State
FIM Full Implicit Method
GPRS General Purpose Research Simulator, in-house simulator of Stanford University
PCA Principal Component Analysis
PE Phase Equilibrium
RV Redeced Variable
PSA Phase -Stability Analysis
SSI Successive Substitution Iteration
TPD Tangent Plane Distance
TPF Two-phase Flash

Acknowledgements

The finical support of the work from the industrial Affiliates programs: Reservoir Simulation, Advanced Well and Smart Fields of Stanford University is greatly appreciated. We also thank Denis Voskov and Alireza Iranshahr at Stanford University for the valuable discussions on CSAT implementation in GPRS.

References

Cao H. 2002 Development of Techniques for General Purpose Simulators, Ph.D. Thesis, Stanford University.

Coats, K. H. 1985 Simulation of Gas Condensate Reservoir Performance. *J. Pet Tech* **Oct.** 1870-1886.

Coats, K.H., Thomas, L.K. and Pierson, R.G.: 1998 Compositional and Black-Oil Reservoir Simulation, *SPE Res Eval & Eng* **1**(4): 372-279.

Firoozabadi, A. and Pan, H. 2002 Fast and Robust Algorithm for Compositional Modeling: Part I-Stability Analysis Testing. *SPE J.* **7**(1): 79-89.

Gong, B., Karimi-Fard, M., Durlofsky, L.J. 2007 An Upscaling Procedure for Constructing Generalized Dual-porosity/dual-permeability Models from Discrete Fracture Characterizations, Paper SPE 102491 presented at the SPE Annual Technical Conference and Exhibition, San Antonio, 24-27 September.

Hendriks, E.M. and van Bergen, A.R.D. 1992 Application of a Reduction Method to Phase Equilibria Calculations. *Fluid PhaseEquilibria* **74**: 17-34.

Honami, Y., Arihara, N., and Yazawa, N. 2000 Accuracy and Efficiency Evaluation of EOS Computation Methods for Compositional Simulation. Paper SPE 59428 presented at SPE Asia Pacific Conference on Integrated Modelling for Asset Management, Yokohama, Japan, 25-26 April.

Hoteit, H. and Firoozabadi, A. 2006 Simple Phase Stability-Testing Algorithm in the Reduction Method. *AIChE J.* **52**(8): 2909-2920.

Jensen, B.H. and Fredenslund, A. 1987 A Simplified Flash Procedure for Multicomponent Mixtures Containing Hydrocarbons and One Non-hydrocarbon Using Two-Parameter Cubic Equations of State. *Industrial & Engineering Chemistry Research* **26**(10): 2129 - 2134.

Jiang Y. 2007 A Flexible Computational Framework for Efficient Integrated Simulation of Advanced Wells and Unstructured Reservoir Models, Ph.D. Thesis, Stanford University.

Kaul, P. and Thrasher, R.L. 1996 A Parameter-Based Approach for Two-phase-equilibrium Prediction with Cubic Equations of State. *SPE Res Eng* **11**(4): 273-279.

Kenyon D., Behie G.A. 1983 Third SPE Comparative Solution Project: Gas Cycling of Retrograde Condensate Reservoirs, Paper SPE 12278 presented at the 7th SPE Symposium on Reservoir Simulation, San Francisco, CA, 15-18 November

Killough J.E., Kossack C.A., 1987 Fifth comparative solution project: evaluation of miscible flood simulators, Paper SPE 16000 presented at the 7th SPE Symposium on Reservoir Simulation, San Antonio, Texas, 1-4 February.

Li, Y. and Johns, R.T. 2006 Rapid Flash Calculations for Compositional Simulation. *SPE Res Eval & Eng* **9**(4): 521- 529.

Michelsen, M.L. 1986 Simplified Flash Calculations for Cubic Equations of State. *Industrial & Engineering Chemistry Process Design and Development* **25**(1): 184-188

Nichita, D.V., Broseta, D., and de Hemptinne, J.-C. 2004 Multiphase Equilibrium Calculation Using Reduced Variables. Paper SPE 89439 presented at SPE/DOE Symposium on Improved Oil Recovery, Tulsa, Oklahoma, 17-21 April.

Okuno, R., Johns, R.T., and Sepehrnoori, K. 2008 Use of a Reduced Method in Compositional Simulation. Paper presented at the 11th European Conference on the Mathematics of Oil Recovery, Bergen, Norway, 8-11 September.

Pan, H. and Firoozabadi, A. 2003. Fast and Robust Algorithm for Compositional Modeling: Part II-Two-phase Flash Computations. *SPE J.* **8**(4): 380-391.

Robinson, D.B. and Peng, D.-Y. 1978 The Characterization of the Heptanes and Heavier Fractions for the GPA Peng-Robinson Programs. Gas Processors Association, Research report RR-28, March, 1978.

Rasmussen C.P., Krejbjerg K., Michelsen M.L., Bjurstrom K.E. 2006 Increaseng of Computational Speed of Flash Calculations with Applications for Compositional, Transient Simulations, *SPE Res Eval & Eng*, **9**(1): 32-38.

Stenby, E.H. and Wang, P. 1993 Noniterative Phase Equilibrium Calculation in Compositional Reservoir Simulation. Paper SPE 26641 presented at SPE Annual Technical Conference and Exhibition, Houston, Texas, 3-6 October.

Voskov, D,V. and Tchelepi, H.A. 2009a Compositional Space Parameterization: Theory and Application for Immiscible Displacements. *SPE J.* **14**(3): 431-440.

Voskov, D,V. and Tchelepi, H.A. 2009b Compositional Space Parameterization: Multicontact Miscible Displacements and Extension to Multiple Phases. *SPE J.* **14**(3): 441-449.

Voskov, D,V. and Tchelepi, H.A. 2009c General Nonlinear Solution Strategies for Multiphase Multicomponent EoS Based Simulation, Paper SPE 118996, presented at SPE Reservoir Simulation Symposium, Woodlands, Texas, 2-4 February.

Wang, P. and Barker, J.W. 1995 Comparison of Flash Calculations in Compositional Reservoir Simulation. Paper SPE 30787 presented at SPE Annual Technical Conference and Exhibition, Dallas, Texas, 22-25 October.